



UNIVERSITAT POLITÈCNICA
DE CATALUNYA

Hybrid model of a doubly-fed induction machine and a back-to-back converter

C. Batlle, A. Dòria-Cerezo, E. Fossas

IOC-DT-P-2005-9
Març 2005



Hybrid model of a doubly-fed induction machine and a back-to-back converter.

C. Batlle^{1,2,4}, A. Dòria-Cerezo⁴, E. Fossas^{3,4}

¹EPSEVG, ²MAIV, ³ESAI, and ⁴IOC

Technical University of Catalonia

January, 2005

Abstract

This report details the port interconnection of two subsystems: a power electronics subsystem (a back-to-back AC/AC converter (B2B), coupled to a phase of the power grid), and an electromechanical subsystem (a doubly-fed induction machine (DFIM), coupled mechanically to a flywheel and electrically to the power grid and to a local varying load). Both subsystems have been essentially described in previous reports (deliverables D 0.5 and D 4.3.1), although some previously unpublished details are presented here. The B2B is a variable structure system (VSS), due to the presence of control-actuated switches; however, from a modelling and simulation, as well as a control-design, point of view, it is sensible to consider modulated transformers (MTF in the bond-graph language) instead of the pairs of complementary switches. The port-Hamiltonian models of both subsystems are presented and coupled through a power-preserving interconnection, and the Hamiltonian description of the whole system is obtained; detailed bond-graphs of all the subsystems and the complete system are provided.

1 Introduction

Doubly-fed induction machines (DFIM) have been proposed in the literature, among other applications, for high performance storage systems [1], wind-turbine generators [9][11] or hybrid engines [3]. The attractiveness of the DFIM stems primarily from its ability to handle large speed variations around the synchronous speed (see [10] for an extended literature survey and discussion). In this work we are interested in the application of DFIM as part of an autonomous energy-switching system that regulates the energy flow between a local prime mover (a flywheel) and the electrical power network, in order to satisfy the demand of a time-varying electrical load, see Figure 1.

The Back-to-back (B2B) converter, connected to and auxiliary single-phase grid, provides the desired PWM rotor voltages to the DFIM. The B2B has the nice feature that power can flow to any direction. In particular for this application, the rotor energy of the DFIM may come back to the converter in some operation ranges [2].

The final goal is to supply the required power to the load with a high network power factor, *i.e.*, $Q_n \sim 0$, where Q_n is the network reactive power. On the other hand, we

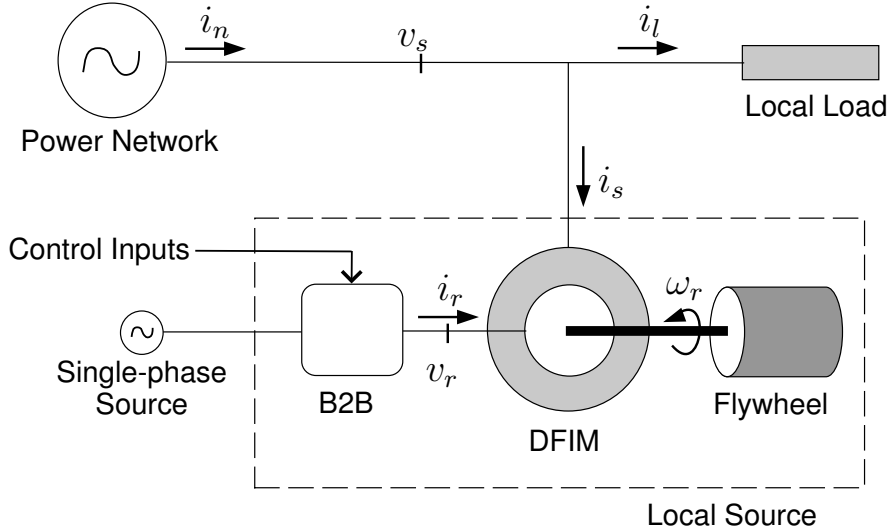


Figure 1: The system: A DFIM coupled to a flywheel connected between a local load and a power grid, controlled by a B2B converter.

require a unity power factor for the single-phase auxiliary grid and a constant value of the DC capacitor link of the B2B.

This report addresses only the modelling aspects of the problem, and in particular the ones related to the interconnection of the two subsystems.

2 Bond Graph and Port-controlled Hamiltonian models

Bond graph theory is a powerful technique to model physical systems [7]. This technique is graphically oriented and represents the power flow between the different elements of a system.

Mathematical equations suitable for simulation can be easily deduced, either manually or using specialized software, from the bond graph representation. This represents a big advantage for complex and/or large systems made of smaller subsystems, since the bond graph description has a “built-in” port description.

Port-controlled Hamiltonian systems (PCHS) can be seen as a mathematical description of bond graphs [6]. An explicit PCHS has the form [4]

$$\begin{cases} \dot{x} = (\mathcal{J}(x) - \mathcal{R}(x))\nabla H(x) + g(x)u \\ y = g^T(x)(\nabla H(x))^T \end{cases} \quad (1)$$

where $x \in \mathbb{R}^n$ are the energy variables, $H(x) : \mathbb{R}^n \rightarrow \mathbb{R}$ is the energy (or Hamiltonian) function¹, $u, y \in \mathbb{R}^m$ are the port variables, $\mathcal{J}(x) = -\mathcal{J}^T(x) \in \mathbb{R}^{n \times n}$ is the interconnection structure matrix, describing how the energy flows inside the system, $0 \leq \mathcal{R} = \mathcal{R}^T \leq 0 \in \mathbb{R}^{n \times n}$ is the dissipation matrix, and $g(x) \in \mathbb{R}^{n \times m}$ is the interconnection matrix, describing the port connection of the system.

Port variables are conjugated, so that $[u][y]$ has units of power.

¹ ∇ operator represents the gradient of the function, and for simplicity is taken as a column vector

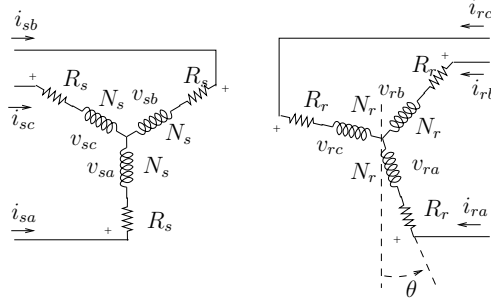


Figure 2: Basic scheme of the doubly-fed induction machine

2.1 The Doubly-fed Induction Machine coupled to a flywheel

Figure 2 shows a scheme of a doubly-fed three-phase induction machine. It contains 6 energy storage elements, with their associated dissipations, and 6 ports (the 3 stator and the 3 rotor voltages and currents).

A Port-controlled Hamiltonian model of a DFIM coupled to a flywheel is given in [2]. This model is described in dq -coordinates [8], which reduces the three-phase variables (abc) to the two-phase variables (dq). The variables are

$$x_D^T = (\lambda_s^T, \lambda_r^T, J_m \omega_r) \in \mathbb{R}^5,$$

or

$$x_D^T = (x_e^T, x_m) = (\Lambda^T, J_m \omega_r)$$

where $\Lambda^T = (\lambda_s^T, \lambda_r^T) \in \mathbb{R}^4$, $\lambda_s, \lambda_r \in \mathbb{R}^2$ are the inductor fluxes in dq -coordinates (stator and rotor respectively), ω_r the angular speed of the rotor, and J_m is the inertia (DFIM+flywheel). The structure and damping matrices are

$$\mathcal{J}_D = \begin{pmatrix} -\omega_s L_s J_2 & -\omega_s L_{sr} J_2 & O_{2 \times 1} \\ -\omega_s L_{sr} J_2 & -(\omega_s - \omega_r) L_r J_2 & L_{sr} J_2 i_s \\ O_{1 \times 2} & L_{sr} i_s^T J_2 & 0 \end{pmatrix} \in \mathbb{R}^{5 \times 5} \quad \mathcal{R}_D = \begin{pmatrix} R_s I_2 & O_{2 \times 2} & O_{2 \times 1} \\ O_{2 \times 2} & R_r I_2 & O_{2 \times 1} \\ O_{1 \times 2} & O_{1 \times 2} & B_r \end{pmatrix} \in \mathbb{R}^{5 \times 5}$$

where L are inductances, R are resistances, lower indices s and r refer to stator and rotor respectively, B_r is the mechanical damping and i_s and $i_r \in \mathbb{R}^2$ are the stator and rotor currents. Currents $i^T = (i_s^T, i_r^T) \in \mathbb{R}^4$ and fluxes λ are related with

$$\Lambda = \mathcal{L}i$$

where the inductance matrix \mathcal{L} is

$$\mathcal{L} = \begin{pmatrix} L_s I_2 & L_{sr} I_2 \\ L_{sr} I_2 & L_r I_2 \end{pmatrix} \in \mathbb{R}^{4 \times 4},$$

and

$$J_2 = \begin{pmatrix} 0 & -1 \\ 1 & 0 \end{pmatrix} \in \mathbb{R}^{2 \times 2} \quad I_2 = \begin{pmatrix} 1 & 0 \\ 0 & 1 \end{pmatrix} \in \mathbb{R}^{2 \times 2}. \quad (2)$$

The interconnection matrix is

$$g_D = \begin{pmatrix} I_2 & O_{2 \times 2} \\ O_{2 \times 2} & I_2 \\ O_{1 \times 2} & O_{1 \times 2} \end{pmatrix} \in \mathbb{R}^{5 \times 4}$$

with the port variables

$$u^T = (v_s^T, v_r^T) \in \mathbb{R}^4,$$

where $v_s, v_r \in \mathbb{R}^2$ are the stator and rotor voltages. Finally, the Hamiltonian (or energy) function is

$$H_D = \frac{1}{2} \Lambda^T \mathcal{L}^{-1} \Lambda + \frac{1}{2J_m} x_m^2.$$

The Bond Graph of the DFIM is depicted in Figure 3.

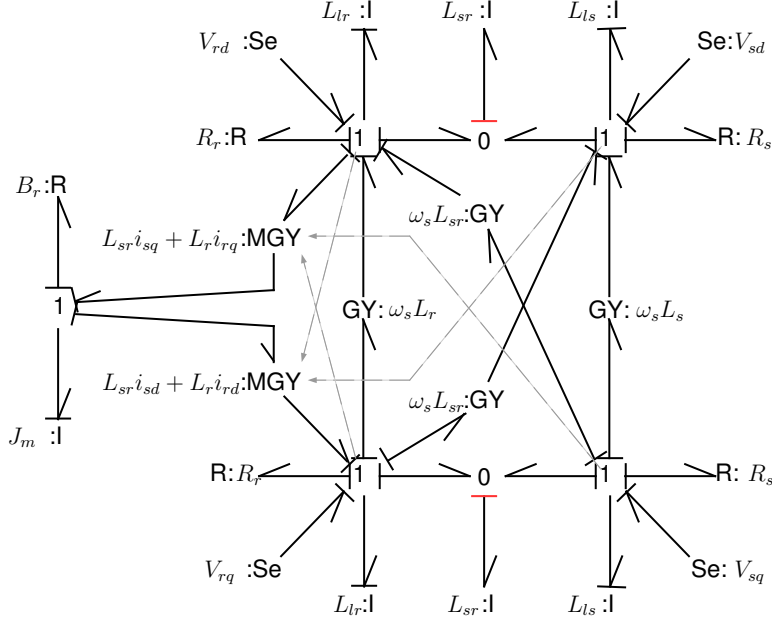


Figure 3: Bond Graph of the DFIM.

2.2 The back-to-back converter

Figure 4 shows a the back-to-back converter. It is made of a full bridge AC/DC single-phase boost-like rectifier and a 3-phase DC/AC inverter. The whole converter has an AC single-phase voltage input and its output are 3-phase PWM voltages which feed the rotor windings of the electrical machine. This system can be split into two parts: a dynamical subsystem (the full bridge rectifier, containing the storage elements), and an static subsystem (the inverter, which, from the energy point of view, acts like a transformer).

$v_i(t) = E \sin(\omega_s t)$ is a single-phase AC voltage source, L is the inductance (including the effect of any transformer in the source), C is the capacitor of the DC part, r takes into account all the resistance losses (inductor, source and switches), s_k and t_k , $k = 1, 2, 4, 5, 6$. Switch states take values in $\{-1, 1\}$ and t -switches are complementary to s -switches: $t_k = \bar{s}_k = -s_k$. Additionally, $s_2 = \bar{s}_1 = -s_1$.

The PCHS averaged model of the full-bridge rectifier is as follows. The Hamiltonian variables are

$$x_B^T = (\lambda_L, q) \in \mathbb{R}^2,$$

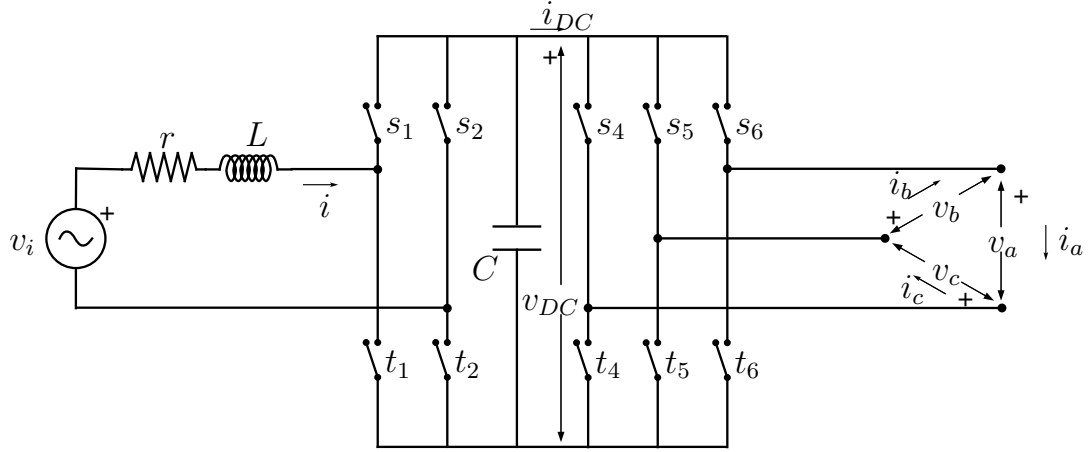


Figure 4: Back-to-back converter.

where $\lambda_L \in \mathbb{R}^2$ is the inductor flux and q is the DC charge in the capacitor. The Hamiltonian function is

$$H_B = \frac{1}{2L}\lambda^2 + \frac{1}{2C}q^2,$$

while the structure and damping matrices are

$$\mathcal{J}_B = \begin{pmatrix} 0 & -s_1 \\ s_1 & 0 \end{pmatrix} \in \mathbb{R}^{2 \times 2} \quad \mathcal{R}_B = \begin{pmatrix} r & 0 \\ 0 & 0 \end{pmatrix} \in \mathbb{R}^{2 \times 2}.$$

The interconnection matrix is

$$g_B = \begin{pmatrix} 1 & O_{1 \times 3} \\ 0 & f^T \end{pmatrix} \in \mathbb{R}^{2 \times 4},$$

where

$$f = \frac{1}{2} \begin{pmatrix} s_6 - s_4 \\ s_5 - s_6 \\ s_4 - s_5 \end{pmatrix} \in \mathbb{R}^3,$$

and

$$u = \begin{pmatrix} v_i \\ -i_{abc} \end{pmatrix} \in \mathbb{R}^4,$$

where $i_{abc}^T = (i_a, i_b, i_c) \in \mathbb{R}^3$ are the three-phase currents in the inverter part. Notice that the inverter subsystem can be seen as a Dirac structure with

$$\begin{aligned} v_{abc} &= f v_{DC} \\ i_{DC} &= f^T i_{abc} \end{aligned}$$

where $v_{abc}^T = (v_a, v_b, v_c) \in \mathbb{R}^3$ are the three-phase voltages and $v_{DC}, i_{DC} \in \mathbb{R}$ are the DC voltage in C and the DC current supplied by the rectifier subsystem.

The Bond Graph model of the B2B converter is depicted in Figure 5. The switch model has been taken as a transformer, which has the same behavior than an ideal switch for an averaged model [5].

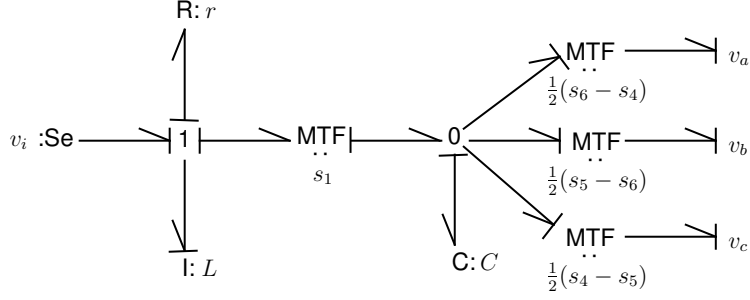


Figure 5: Bond Graph of the B2B converter.

2.3 The dq -transformation

From an analysis point of view it is convenient to express the three-phase inverter voltages of the DFIM in dq components.

We can summarize the dq -transformation as follows. First, from the original three phase electrical variables (voltages, currents, fluxes...) y_{abc} we compute transformed variables $y_{\alpha\beta\gamma}$ by means of

$$y_{\alpha\beta\gamma} = T y_{abc} \quad (3)$$

with

$$T = \begin{pmatrix} t_{11} & t_{12} & t_{13} \\ t_{21} & t_{22} & t_{23} \\ t_{31} & t_{32} & t_{33} \end{pmatrix}.$$

with $T^T = T^{-1}$, so that this is a power-preserving transformation:

$$\langle i, v \rangle = \langle i_{abc}, v_{abc} \rangle.$$

For instance,

$$T = \begin{pmatrix} \frac{\sqrt{2}}{\sqrt{3}} & -\frac{1}{\sqrt{6}} & -\frac{1}{\sqrt{6}} \\ 0 & \frac{1}{\sqrt{2}} & -\frac{1}{\sqrt{2}} \\ \frac{1}{\sqrt{3}} & \frac{1}{\sqrt{3}} & \frac{1}{\sqrt{3}} \end{pmatrix}.$$

For a three-phase equilibrated system, one has $y_a + y_b + y_c = 0$; the dq -transformation allows then working with only the two first components (the $\alpha - \beta$ components) and neglect the third one, the γ , or homopolar, component, which is zero for any balanced set and which, in any case, is dynamically decoupled from the other components.

The second part of the transformation relies on the assumption that the induction machine is symmetric, with a sinusoidal distribution of magnetic fluxes in the air gap. It eliminates the dependence of the equations on θ (mechanical position of the rotor), and consists in defining new variables y_{dq} via

$$\begin{pmatrix} y_{\alpha\beta s} \\ y_{\alpha\beta r} \end{pmatrix} = K(\theta, \delta) \begin{pmatrix} y_{dqs} \\ y_{dqr} \end{pmatrix} \quad (4)$$

$$K(\theta, \delta) = \begin{bmatrix} e^{J_2\delta} & O_2 \\ O_2 & e^{J_2(\delta-\theta)} \end{bmatrix} \in \mathbb{R}^{6 \times 6}$$

where δ is an arbitrary function of time, and

$$e^{J_2\phi} = \begin{pmatrix} \cos(\phi) & -\sin(\phi) \\ \sin(\phi) & \cos(\phi) \end{pmatrix} \in \mathbb{R}^{2 \times 2}.$$

If $\dot{\delta}$ is the stator frequency ω_s , this has the nice additional property of converting the sinusoidal time-dependent stator variables into constant values, which is useful for controlling purposes [2].

Notice that this transformation can be seen as a Dirac structure [4],

$$v_{abc} = K(\theta, \delta)T v_{dq} \quad (5)$$

$$i_{dq} = -(K(\theta, \delta)T)^T i_{abc}. \quad (6)$$

For the rotor part, one has $K_r(\theta, \delta) = e^{J_2(\delta-\theta)}$.

The dq-transformation can be seen, in bond graph terms, as a modulated transformation in two steps, figure (6). First the T transformation reduces, in an equilibrated case, from a 3-phase (abc) to a 2-phase ($\alpha\beta$). Then $K(\delta, \theta)$ simplifies the dynamical equations of the DFIM.

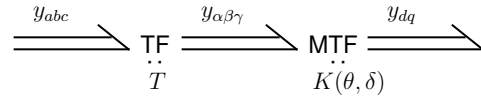


Figure 6: Bond graph of the dq-transformation.

Fig.(7) shows a completed bond graph of the first step of the dq -transformation. Indeed, we write the output equations for efforts

$$\begin{aligned} e_\alpha &= t_{11}e_a + t_{12}e_b + t_{13}e_c \\ e_\beta &= t_{21}e_a + t_{22}e_b + t_{23}e_c \\ e_\gamma &= t_{31}e_a + t_{32}e_b + t_{33}e_c. \end{aligned} \quad (7)$$

which implement (3). For the flows we have (10)

$$\begin{aligned} f_\alpha &= \frac{1}{t_{11}}f_{a1} = \frac{1}{t_{12}}f_{b1} = \frac{1}{t_{13}}f_{c1} \\ f_\beta &= \frac{1}{t_{21}}f_{a2} = \frac{1}{t_{22}}f_{b2} = \frac{1}{t_{23}}f_{c2} \\ f_\gamma &= \frac{1}{t_{31}}f_{a3} = \frac{1}{t_{32}}f_{b3} = \frac{1}{t_{33}}f_{c3} \end{aligned} \quad (8)$$

$$\begin{aligned} f_a &= f_{a1} + f_{a2} + f_{a3} \\ f_b &= f_{b1} + f_{b2} + f_{b3} \\ f_c &= f_{c1} + f_{c2} + f_{c3}, \end{aligned} \quad (9)$$

and finally

$$f_{abc} = T^T f_{\alpha\beta\gamma}, \quad (10)$$

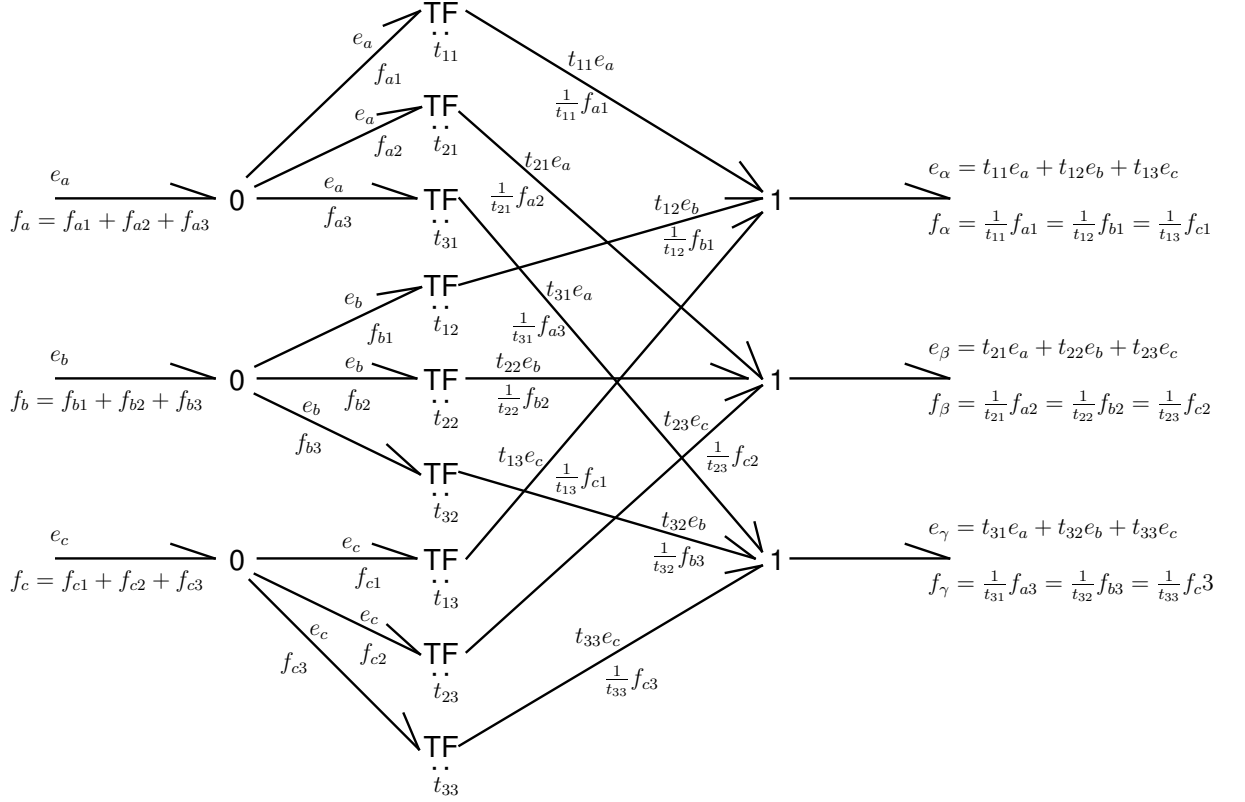


Figure 7: Completed bond graph of the dq-transformation.

which, expressed in $\alpha\beta\gamma$ -components, is

$$f_{\alpha\beta\gamma} = (T^T)^{-1} f_{abc}. \quad (11)$$

Since $T^T = T^{-1}$ we recover expression (3) for flows. Note that for an equilibrated 3-phase system the bond graph takes a form where the γ -port disappears, Fig.(8). For the second part of the transformation, the bond graph is shown in Fig.(9). Following the same steps as for the first part of the transformation, we recover (4), since $e^{-J_2\phi} = (e^{J_2\phi})^T$.

Finally the complete dq -transformation is depicted in Fig.(10), with a 3-input port (abc) and a 2-output port(dq).

2.4 PCH model of the whole system

Figure 11 shows the interconnection scheme of the whole system (B2B+DFIM). The dq -transformation connects the B2B converter with the DFIM as a Dirac structure.

The interconnection relations are

$$\begin{aligned} v_r &= v_{dq} \\ i_r &= i_{dq} \\ v_{ABC} &= v_{abc} \\ i_{ABC} &= i_{abc}. \end{aligned}$$

We use equation (12) and introduce a new \mathcal{K} matrix

$$\mathcal{K} = T_*^T K \in \mathbb{R}^{2 \times 3},$$

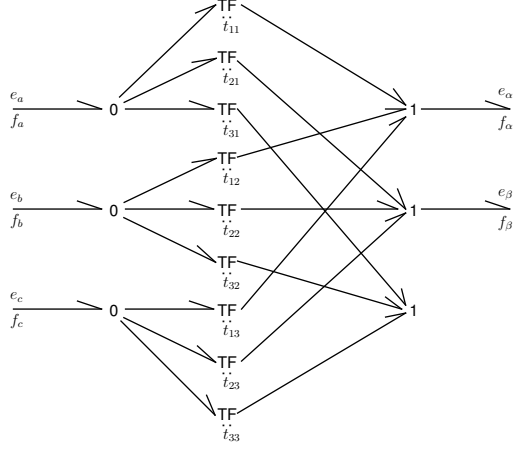


Figure 8: Reduced bond graph of the dq -transformation for an equilibrated system.

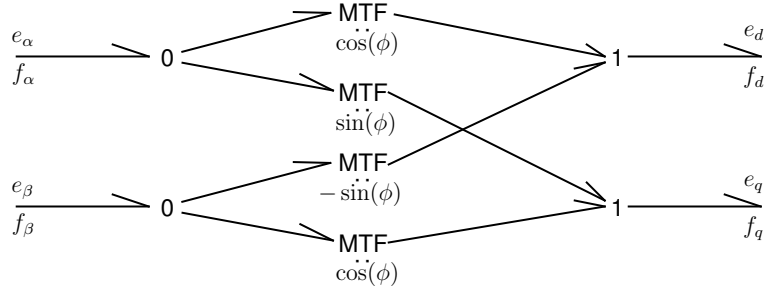


Figure 9: Bond graph of the dq -transformation.

with T_* defined so as to remove the homopolar component:

$$T_* = \begin{pmatrix} \frac{\sqrt{2}}{\sqrt{3}} & -\frac{1}{\sqrt{6}} & -\frac{1}{\sqrt{6}} \\ 0 & \frac{1}{\sqrt{2}} & -\frac{1}{\sqrt{2}} \end{pmatrix} \in \mathbb{R}^{2 \times 3}.$$

The PCHS of the whole system has the following variables

$$x^T = (\Lambda^T, J_m \omega_r, \lambda, q) \in \mathbb{R}^7$$

with energy function

$$H = H_D + H_B = \frac{1}{2} \Lambda^T \mathcal{L}^{-1} \Lambda + \frac{1}{2J_m} x_m^2 + \frac{1}{2L} \lambda^2 + \frac{1}{2C} q^2.$$

The structure and dissipation matrices are

$$\mathcal{J} - \mathcal{R} = \begin{pmatrix} & & & O_{2 \times 1} & O_{2 \times 1} \\ & \mathcal{J}_D - \mathcal{R}_D & & O_{2 \times 1} & \mathcal{K}f \\ & & & 0 & 0 \\ O_{1 \times 2} & O_{1 \times 2} & 0 & & \\ O_{1 \times 2} & -f^T \mathcal{K}^T & 0 & \mathcal{J}_B - \mathcal{R}_B & \end{pmatrix} \in \mathbb{R}^{7 \times 7}$$

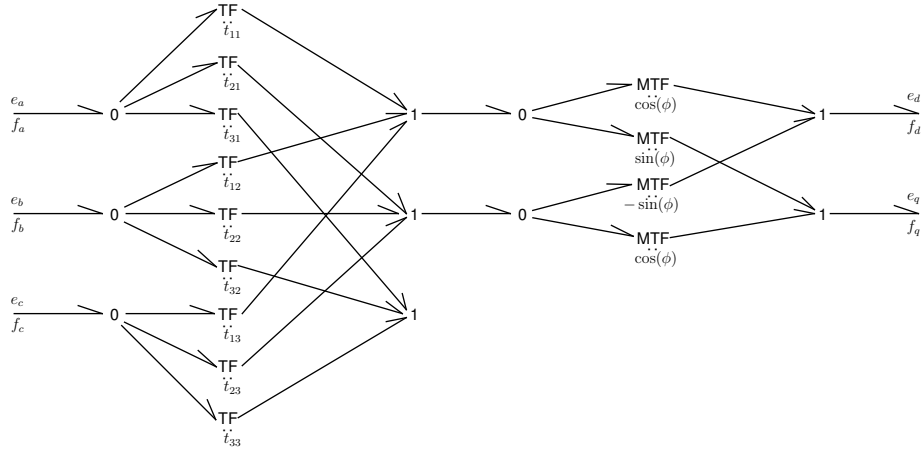


Figure 10: Complete bond graph of the dq -transformation.

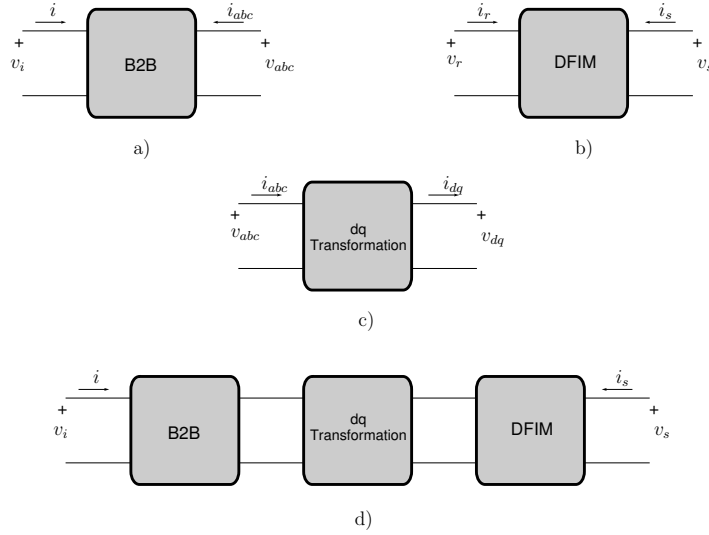


Figure 11: Interconnection scheme.

and the interconnection matrix and port variables are

$$g = \begin{pmatrix} I_2 & O_{2 \times 1} \\ O_2 & O_{2 \times 1} \\ O_{1 \times 2} & 0 \\ O_{1 \times 2} & 1 \\ O_{1 \times 2} & 0 \end{pmatrix} \in \mathbb{R}^{7 \times 3} \quad u^T = (v_s^T, v_i) \in \mathbb{R}^3.$$

The bond graph of the whole system is shown in Figure 12.

References

- [1] H. Akagi and H. Sato. Control and performance of a doubly-fed induction machine intended for a flywheel energy storage system. *IEEE Trans. Power Electron.*, (17):109–116, 2002.

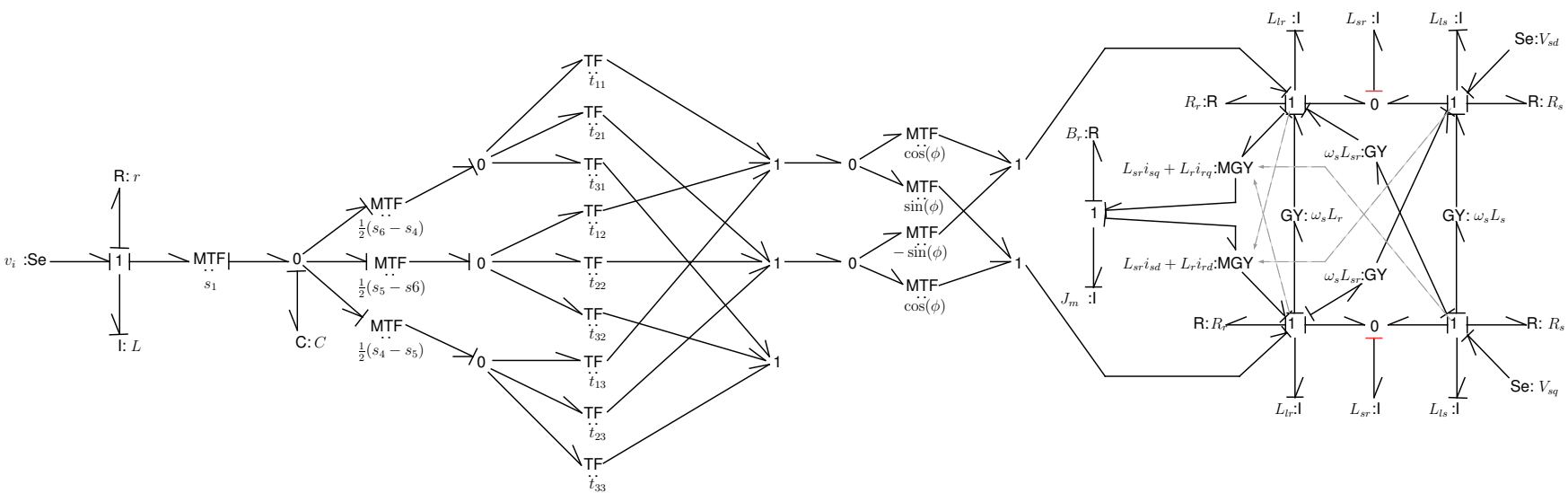


Figure 12: Bond graph representation of the whole system.

- [2] C. Batlle, A. Dòria-Cerezo, and R. Ortega. Power Flow Control of a Doubly-Fed Induction Machine Coupled to a Flywheel. In *IEEE Proc. Conference on Control Applications*, pages 1645–1651, 2004.
- [3] P. Caratozzolo, E. Fossas, J. Pedra, and J. Riera. Dynamic modeling of an isolated motion system with DFIG. In *Proc. CIEP*, pages 287–292, 2000.
- [4] M. Dalsmo and A. van der Schaft. On representations and integrability of mathematical structures in energy-conserving physical systems. *SIAM J. Control Optim.*, (37):54–91, 1998.
- [5] M. Delgado and H. Sira-Ramirez. Modeling and simulation of a switch regulated DC-to-DC power converters of the boost type. In *IEEE Proc. Conf. on Devices, Circuits and Systems*, pages 84–88, 1995.
- [6] G. Golo, A.J. van der Schaft, P.C. Breedveld, and B. Maschke. Hamiltonian formulation of Bond Graphs. In *Workshop NACO II*, pages 2642–2647, 2001.
- [7] D.C. Karnopp, D.L. Margolis, and R.C. Rosenberg. *System dynamics modeling and simulation of mechatronic systems*. J. Wiley, New York, 3th edition, 2000.
- [8] P. C. Krause. *Analysis of electric machinery*. McGraw-Hill, 1986.
- [9] R. Peña, J. C. Clare, and G. M. Asher. Doubly fed induction generator using back-to-back pwm converters and its application to variable speed wind-energy generation. In *IEEE Proc. Electric Power Applications*, number 143, pages 231–241, 1996.
- [10] S. Peresada, A. Tilli, and A. Tonelli. Power control of a doubly fed induction machine via output feedback. *Control Engineering Practice*, (12):41–57, 2004.
- [11] J.G. Slootweg, H. Polinder, and W.L. Kling. Dynamic modelling of a wind turbine with doubly fed induction generator. In *IEEE Power Engineering Society Summer Meeting 2001*, pages 644–649, 2001.